

by: Dr. Juan F. Lara
Center for Relativity
University of Texas at Austin

Motivation

- Certain baryogenesis models lead to inhomogeneous baryon distributions.
- Isotope abundance observations are increasing in accuracy. Small corrections such as the neutrino heating effect might be measurable.
- The neutrino heating effect has not been calculated for an inhomogeneous model of the universe. The results might defer from standard model results.

THE BARYON INHOMOGENEOUS BIG BANG NUCLEOSYNTHESIS MODEL

This Inhomogeneous Big Bang Nucleosynthesis (IBBN) model is a spherically symmetric model that initially has a high neutron and proton density inner region and a low density outer region. A first-order quark-hadron phase transition (MM 1993) is a baryogenesis model that can produce such a distribution. The baryon-to-photon ratio η and the distance scale r_i , the radius of the whole model at the run's initial temperature $T = 100$ GK. The boundary r_b between high and low density regions is at $1/2r_i$ and the ratio between the densities $R_\rho = 800$.

The model is broken up into a core and 63 spherical shells. The number density $n(i, s)$ for isotope i in shell s evolves according to this equation. (Kaimulainen et al, 1998)

$$\frac{dn(i, s)}{dt} = \frac{1}{n_b(s)} \sum_{j,k,l} N_i \left(-\frac{n^{N_i}(i, s) n^{N_j}(j, s)}{N_i! N_j!} [ij] + \frac{n^{N_k}(k, s) n^{N_l}(l, s)}{N_k! N_l!} [kl] \right) - 3\dot{a}n(i, s) + \frac{1}{r^2} \frac{\partial}{\partial r} \left(r^2 D_n \frac{\partial n(i, s)}{\partial r} \right) \quad (1)$$

The first term corresponds to nuclear reactions within shell s , the second term for the expansion of the universe, and the third term accounts for diffusion between shells. This model has only neutron diffusion, determined by the neutron diffusion coefficient D_n (Kurki-Suonio et al, 1992). $z = m_e/kT$.

$$\frac{1}{D_n} = \frac{1}{D_{ne}} + \frac{1}{D_{np}} \quad (2)$$

$$D_{ne} = \frac{3}{8} \sqrt{\frac{\pi}{2}} \frac{c}{n_e \sigma_{ne}} \frac{K_2(z)}{\sqrt{z} K_{5/2}(z)} \left(1 - \frac{n_n}{n_t} \right) \quad (3)$$

$$D_{np} = \frac{3\sqrt{\pi}}{4} \sqrt{\frac{kT}{m_p}} \frac{c}{n_p \sigma_{np}} \left(1 - \frac{n_n}{n_t} \right) \quad (4)$$

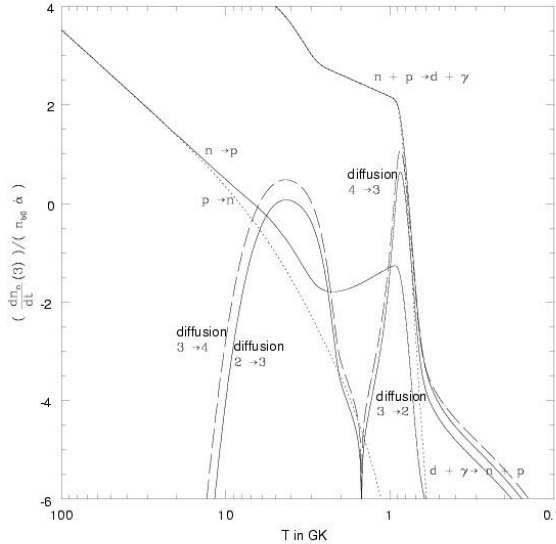


Figure (2): Neutron diffusion and back diffusion rates into and out of shell 3, compared with the neutron-proton conversion rates in shell 3 and the nuclear reaction rate $n + p \leftrightarrow d + \gamma$. $r_i = 25000$ cm.

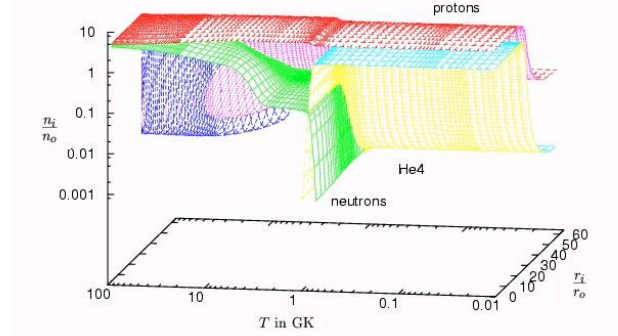
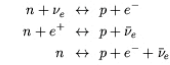


Figure (1): Neutron, proton and ${}^4\text{He}$ number densities for $r_i = 25000$ cm. Neutrons homogenize while protons remain concentrated in the inner regions. Back diffusion leads to ${}^4\text{He}$ production overwhelmingly in the inner shells.

$r_i = 25000$ cm and $\eta = 5.1 \times 10^{-10}$ for the following figures. Figure (1) above shows $n(i, j)$ for neutrons, protons, and ${}^4\text{He}$ nuclei. Initially weak reactions



interconvert neutrons and protons leading to an overall increase in protons in all shells. But from the boundary outwards neutrons diffuse from the high density shells to the low density shells. In Figure (1) the neutron distribution is homogenized by the time when temperature $T = 2$ GK. Nucleosynthesis occurs around $T = 0.9$ GK. Nucleosynthesis happens slightly earlier in the inner shells because of the higher proton density, depleting neutrons sooner. Neutrons from the outer shells back diffuse to the inner shells and nucleosynthesis happens primarily in the inner shells. ${}^4\text{He}$ has a high number density in the inner shells.

Figure (2) on the left shows the reaction rates that change the neutron number density $n(n, 3)$ in shell 3, a high density inner shell. Neutron diffusion becomes significant in this shell at $T =$ around 4 GK, some time after the neutron-proton interconversion reactions have fallen out of equilibrium. The nuclear reaction rate $n + p \leftrightarrow d + \gamma$ falls out of equilibrium at $T = 0.9$ GK and that is when production of deuterium and heavier elements becomes significant. Neutron back diffusion peaks at 0.9 GK as well.

THE NEUTRINO HEATING EFFECT

Electrons and positrons annihilate during temperatures $T = 5$ GK down to 1 GK. e^-e^+ pairs can create $\nu\bar{\nu}$ pairs, and electrons and positrons scatter off of neutrinos. These reactions transfer energy from electrons and positrons to neutrons. The distribution functions $f_i = f(p_i)$ of electron (μ, τ) neutrinos evolve according to the Boltzmann Transport Equation. (Hannestad & Madsen, 1996).

$$\frac{df_1}{dt} = C_{coll} \quad (5)$$

$$C_{coll} = \frac{1}{2E_1} \left(\frac{kT_N}{R} \right)^5 \int \frac{d^3p_2}{(2\pi)^3 2E_2} \int \frac{d^3p_3}{(2\pi)^3 2E_3} \int \frac{d^3p_4}{(2\pi)^3 2E_4} S|M|^2 (2\pi)^4 \delta^4(p_1 + p_2 - p_3 - p_4) \Lambda(f_1, f_2, f_3, f_4)$$

$$\Lambda(f_1, f_2, f_3, f_4) = \{ [1 - f_1(p_1)][1 - f_2(p_2)]f_3(p_3)f_4(p_4) - f_1(p_1)f_2(p_2)[1 - f_3(p_3)][1 - f_4(p_4)] \}$$

The matrix elements of the annihilation and scattering reactions with electrons and positrons, as well as scattering reactions between neutrinos, are accounted for in $S|M|^2$. The positive part of Λ corresponds to reactions with the neutrino as an final particle. The negative is for reactions with the neutrino as an initial particle.

Neutrino heating increases the values of the neutrino distribution functions f_i and that increases the neutrino energy densities ρ_{ν_i} . Heating takes that energy away from the electron and positron energy densities ρ_e . The higher energy neutrinos speed up the reaction ($n + \nu_e \rightarrow p + e^-$) but the lower energy positrons slow down ($n + e^+ \rightarrow p + \bar{\nu}_e$).

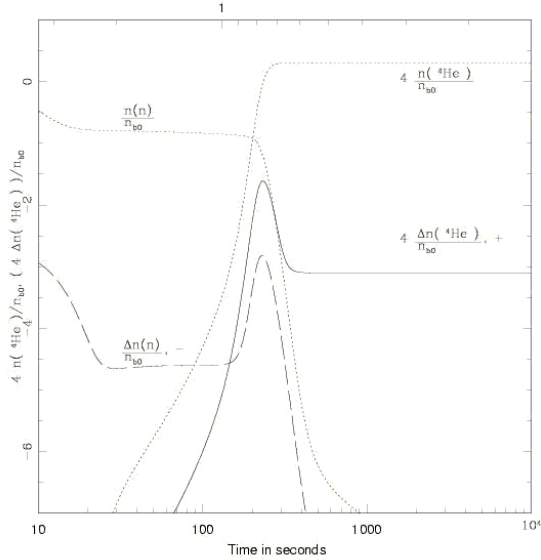


Figure (4): The neutron number density is lower due to neutrino heating. But the clock effect makes nucleosynthesis occur earlier. ${}^4\text{He}$ then has a slightly higher number density.

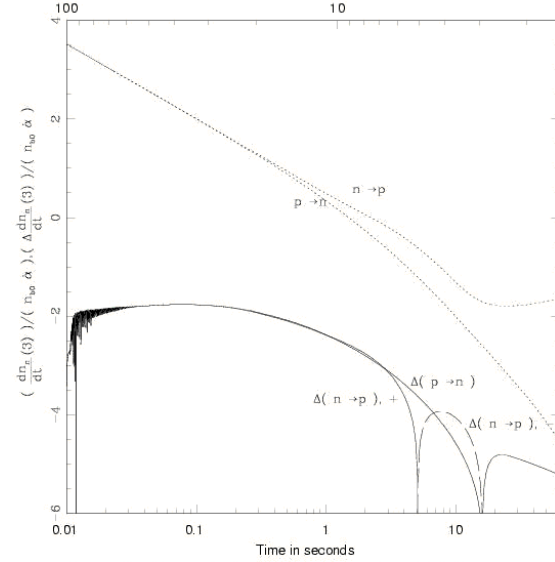


Figure (3): Neutrino heating slightly increases the rates that interconvert neutrons and protons in shell 3, and heating also makes neutron diffusion occur slightly sooner. $r_i = 25000$ cm.

Figure (3) above shows that both the $n \rightarrow p$ and the $p \rightarrow n$ in weak reaction rates increase in nearly equal amounts due to neutrino heating. But as the $p \rightarrow n$ reaction rate falls the $n \rightarrow p$ dominates. The increase in the $n \rightarrow p$ reaction rate prevails at $T = 2$ GK (time $t =$ about 30 seconds), leading to a decrease in the neutron number density.

The decrease in the e^-e^+ energy density also lowers the temperature T at any given time. The lower temperature affects the diffusion coefficient D_{ν} causing neutron diffusion to occur slightly earlier. Earlier diffusion leads to the change in the $n \rightarrow p$ reaction rate in Figure (3) turning negative briefly, neutrons having been depleted slightly sooner.

In Figure (4) on the left neutrino heating has decreased the neutron number density at the time of nucleosynthesis. But because heating decreases the temperature with respect to time nucleosynthesis at $T = 0.9$ GK will occur sooner. This earlier nucleosynthesis is known as the clock effect. At this sooner time the neutron number density is higher then without heating. The clock effect leads to an increase in the final value of the ${}^4\text{He}$ number density. This increase $\Delta n({}^4\text{He}, 3)$ peaks at the time of nucleosynthesis and levels off when $n({}^4\text{He}, 3)$ reaches its final value. The width of the peak is an indicator of the clock effect.

The Change in ${}^4\text{He}$ Due to Neutrino Heating

Figure (5) to the right shows X_{He} , the final mass fraction of ${}^4\text{He}$ for the ranges η from 1 to 30×10^{-10} and r_i from 100 to 10^8 cm. At the values $\eta = 5.1 \times 10^{-10}$ and $r_i = 25000$ cm $X_{\text{He}} = 0.249264$. The contours in Figure (5) depend on when neutron diffusion occurs compared with the neutron-proton interconversion rates and with nucleosynthesis. For the lowest values of r_i diffusion occurs when the interconversion reactions are still in equilibrium, and those reactions plus diffusion can redistribute protons along with neutrons. But as r_i increases diffusion occurs later, and fewer protons are redistributed. With more protons remaining in the inner shells nucleosynthesis occurs there earlier and ${}^4\text{He}$ increases. There comes a value of r_i when diffusion occurs after the interconversion rates have fallen out of equilibrium, leaving all protons in their original shells. X_{He} peaks when that happens. But as r_i increases further back diffusion occurs more slowly and not all neutrons diffuse back before nucleosynthesis ends. ${}^4\text{He}$ starts decreasing as a result. X_{He} bottoms out when neutron diffusion coincides with nucleosynthesis. For higher r_i the inner shells retain most of their neutrons, leading to very large ${}^4\text{He}$ production. For $\eta = 5.1 \times 10^{-10}$ $X_{\text{He}} = 0.244675$ for a low $r_i = 100$ cm, increases to 0.249264 when $r_i = 25000$ cm, then descends to 0.239450 when $r_i = 7.9 \times 10^5$ cm, and increases for r_i higher on.

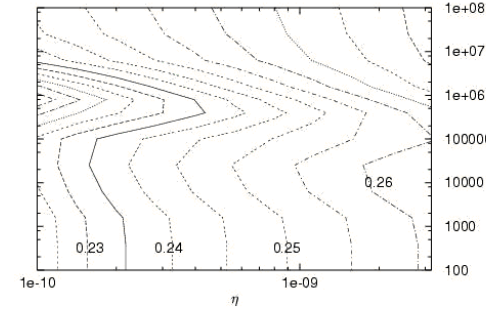


Figure (5): X_{He} is on the order of 0.25. The contours in this graph depend on when neutron diffusion occurs.

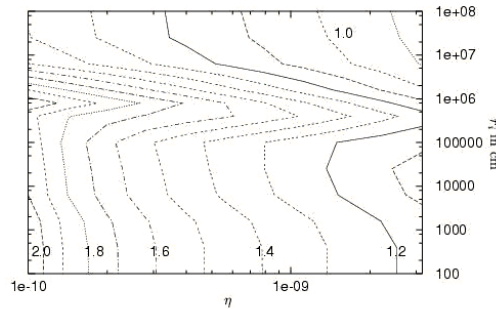


Figure (6): $10^4 \times \Delta X_{\text{He}}$ due to Neutrino Heating. The contours resemble the contours for X_{He} itself in Figure (5).

Figure (6) to the left shows the increase ΔX_{He} in the ${}^4\text{He}$ mass production due to neutrino heating. Through the range of η and r_i the increase is on the order of 10^{-4} . At the values $\eta = 5.1 \times 10^{-10}$ and $r_i = 25000$ cm for instance X_{He} increases by 1.40×10^{-4} , to 0.249404. Increasing the baryon-to-photon ratio makes nucleosynthesis occur earlier, reducing the clock effect. So ΔX_{He} decreases with increasing η_0 . The contours in Figure (6) roughly track the contours in Figure (5). ΔX_{He} decreases when there is greater ${}^4\text{He}$ production and increases when ${}^4\text{He}$ production goes down. The neutrino heating effect on X_{He} is comparable to the effect of increasing η on the order of 1 %.

The Change in Deuterium Due to Neutrino Heating

In Quasi-Stellar objects the ratio of the abundance $Y(d)$ of deuterium to the abundance $Y(p)$ of protons (^1H) is measured. Figure (7) to the right shows $\log[Y(d)/Y(p)]$ for the ranges η from 1 to 30×10^{-10} and r_i from 100 to 10^8 cm. $\log[Y(d)/Y(p)] = -4.64228$ for $\eta = 5.1 \times 10^{-10}$ and $r_i = 25000$ cm. Before nucleosynthesis $Y(d)$ steadily increases. Then $Y(d)$ falls as many nuclear reactions incorporate deuterium to heavier nuclei. Increasing η makes nucleosynthesis earlier. $Y(d)$ is then smaller when nucleosynthesis occurs. $Y(d)/Y(p)$ then decreases as η increases. Figure (7) also tracks Figure (5), with $Y(d)/Y(p)$ decreasing whenever X_{He} increases. For the largest values of r_i shown the high and low density regions behave independently. Regions with baryon-to-photon ratios lower than 10^{-10} can produce considerably more deuterium than regions with larger η . $Y(d)/Y(p)$ is particularly large for these larger values of r_i in Figure (7).

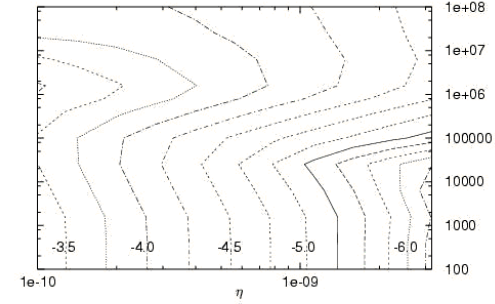


Figure (7): $\log[Y(d)/Y(p)]$ has a range of -3.5 down to -6.0. The contours track the contours of X_{He} in Figure (5), with $\log[Y(d)/Y(p)]$ decreasing when X_{He} increases.

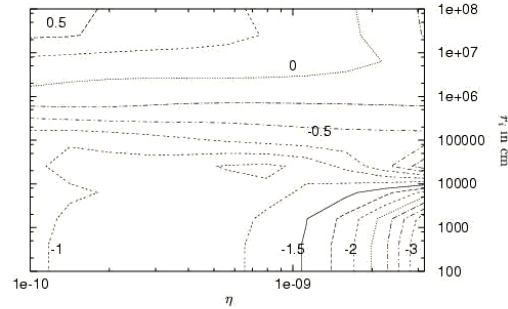


Figure (8): $10^3 \times \Delta(\log[Y(d)/Y(p)])$ due to Neutrino Heating. Large production of deuterium for $r_i > 10^5$ cm leads to an increase rather than a decrease in $\log[Y(d)/Y(p)]$.

Figure (8) to the left shows the change $\Delta(\log[Y(d)/Y(p)])$ for the same ranges of η and r_i as shown in Figure (7). For r_i less than 10^5 cm the change is a decrease on the order of 10^{-3} . For $\eta = 5.1 \times 10^{-10}$ and $r_i = 25000$ cm $\log[Y(d)/Y(p)] = -4.64353$, a decrease of -1.25×10^{-3} . In contrast when η is increased by 1 % the decrease in $\log[Y(d)/Y(p)]$ is around 10^{-2} , an order of magnitude more. These differing results can be used to distinguish the neutrino heating effect from a simple increase in η in isotope abundance measurements. For r_i larger than 10^5 cm the large production of deuterium in the low density region leads to an increase of $\log[Y(d)/Y(p)]$ due to heating.

Future Research

- A journal article on neutron diffusion in this IBBN model is pending.
- A journal article on the neutrino heating effect in the IBBN model will follow. The article will explain the heating effect in further detail for values of r_i other than 25000 cm, particular how the effect influences deuterium.
- The inhomogeneous BBN model can be modified to include more details such as ion diffusion. (Keihanen, 2002) The model can also be used to look at BBN with antimatter regions present. (Giovanni et al, 2002)
- The research in solving the Boltzmann Transport Equation can be applied to calculating the effective neutrino number (Steigman, 2001), or the research can be applied to neutrino transport in element synthesis in stars and supernovae. (Thieleman et al, 2001)

Sources

- Burles, S., Tytler, D. *Astrophysical Journal*. **507**, 732 (1998).
- Giovannini, Massimo, Keihanen, E., Kurki-Suonio, H. *Physical Review D*. **66**, 043504 (2002).
- Hannestad, S., Madsen, J. *Physical Review D*. **54**, 7894 (1996).
- Kainulainen, K., Kurki-Suonio, H., Sihvola, E. *Physical Review D* **59** 083505 (1999).
- Keihanen, E. *Physical Review D*. **66**, 043512 (2002).
- Kurki-Suonio, H., Aufderheide, M.B., Graziani, F., Mathews, G.J., Banerjee, B., Chitre, S.M., Schramm, D.N. *Physics Letters B*. **289**, 211 (1992).
- Malaney, R.A., Mathews, G.J. *Physics Reports*. **229**, 147 (1993).
- Steigman, G. *astro-ph/0108148*
- Thielemann, F-K., Brachwitz, F., Freiburghaus, C., Kolbe, E., Martinez-Pinedo, G., Rauscher, T., Rembges, F., Hix, W.R., Liebendoefer, M., Mezzacappa, A., Kratz, K-L., Pfeiffer, B., Langanke, K., Nomoto, K., Rosswog, S., Schatz, H., Wiescher, M. *Progress in Particle and Nuclear Physics*. **46**, 5 (2001).